PHYSICAL REVIEW B **79**, 100104(R) (2009)

Thermal conductivity and heat capacity of the relaxor ferroelectric $[PbMg_{1/3}Nb_{2/3}O_3]_{1-x}[PbTiO_3]_x$

Makoto Tachibana and Eiji Takayama-Muromachi
National Institute for Materials Science, Namiki 1-1, Tsukuba, Ibaraki 305-0044, Japan
(Received 25 December 2008; published 18 March 2009)

The evolution of thermal conductivity and heat capacity for the series of $[PbMg_{1/3}Nb_{2/3}O_3]_{1-x}[PbTiO_3]_x$ (PMN-PT_x) single crystals with $0 \leq x \leq 1$ are reported. PMN shows typical glasslike behavior in both measurements, which is attributed to the presence of polar nanoregions. With PT doping up to the region of morphotropic phase boundary (MPB), the plateau in thermal conductivity is progressively suppressed. This is reminiscent of partially crystallized glasses and suggests enhanced thermal boundary resistance from ferroelectric domains. The linear temperature contribution and large C_p/T^3 peak in heat capacity remain nearly constant for PT doping up to the MPB but are rapidly suppressed for larger x. These results demonstrate that thermal properties are intimately coupled to the local structures in relaxor ferroelectric systems.

DOI: 10.1103/PhysRevB.79.100104 PACS number(s): 65.40.Ba, 63.50.−x, 66.70.−f, 77.84.Dy

Relaxor ferroelectrics, such as $PbMg_{1/3}Nb_{2/3}O_3$ (PMN) and $PbZn_{1/3}Nb_{2/3}O_3$ (PZN), are technologically important materials with extraordinary dielectric and piezoelectric properties.[1] Relaxors are also important from a basic scientific point of view, as they provide a setting in which to study the role of nanoscale phase inhomogeneities on emergent properties, a feature that is shared by high-temperature superconductors and colossal magnetoresistive materials.[2] Relaxors show a broad and frequency-dependent peak in the dielectric constant (T_{max}=265 K at 1 kHz in PMN), with no long-range ferroelectric order. These behaviors have been linked to the polar nanoregions (PNRs), which begin to develop below ~620 K in PMN and are associated with quenched chemical disorder in these materials. An important aspect of PMN and PZN is that structural and ferroelectric properties can be tuned by doping the normal ferroelectric $PbTiO_3$ (PT). In the solid solution system of $PMN_{(1-x)}$-PT_x (PMN-PT_x for short), one finds the evolution of low-T structure from cubic to rhombohedral, monoclinic, and tetragonal with increasing x. The largest piezoelectric responses are found in the small region of monoclinic phase with $x \approx 0.30-0.35$,[3] which is also referred to as the morphotropic phase boundary (MPB) separating the relaxorlike rhombohedral phase from the ferroelectric tetragonal phase. However, these changes in the average lattice structure are not necessarily correlated with the local polar structures,[1] and detailed mechanism behind the exceptional dielectric and piezoelectric properties remains controversial.[4] Clearly, an important goal is to understand the relationship between the composition, PNRs, and enhanced material properties in these compounds.

Structural studies on PMN have established that this compound remains cubic down to the lowest T, but with two kinds of nanoscale structures. There are chemically ordered regions of Mg^{2+} and Nb^{5+} with a size of ~2–5 nm,[1] and PNRs with rhombohedral symmetry become ~6 nm in size and occupy about 30% of the crystal.[5] Upon PT doping, the substitution of Ti^{4+} for Mg^{2+}/Nb^{5+} suppresses the chemically ordered regions and enhances the size of PNRs, the latter resulting in the breaking of global symmetry from the pseudocubic phase. However, it remains a challenge to describe the structure in the entire length scale, as PNRs coexist with submicrometer-scale ferroelectric domains, and the size and shape of these entities evolve in a complex manner with PT doping.[6,7] [The reported boundary between the cubic and rhombohedral phases varies from $x \sim 0.05$ to 0.27 (Refs. 8 and 9) and depends in part on the experimental probe.] Moreover, there is increasing evidence that PNRs persist into the monoclinic phase,[1] implying that local polarization plays important roles in the enhanced piezoelectric properties. It is for these reasons that better understanding of the inhomogeneous structures of PMN-PT_x is expected to provide important insights on its extraordinary functional properties.

In this Rapid Communication, we present measurements of thermal conductivity κ and heat capacity C_p for the series of single-crystalline PMN-PT_x, which provide unique perspectives on the nanoscale inhomogeneities in this system. These measurements were motivated by earlier work,[10] which established the thermal properties of PMN to be virtually identical to those of glasses or amorphous materials, while PT was found to show a clear example of typical crystalline behavior. Therefore, by studying the manner in which the glasslike behavior in PMN is transformed into crystalline behavior with PT doping, we can obtain insights on how PNRs are transformed into macroscopic polarization. The results show interesting correlation with the phase diagram of PMN-PT_x and demonstrate that inhomogeneous structures have significant influence on the thermal properties of relaxor ferroelectric systems.

Single crystals of PMN-PT_x with x=0, 0.07, 0.27, 0.56, 0.79, 0.89, and 1 were grown by the flux method using PbO and B_2O_3 as the flux. For each x, rectangular parallelepiped crystals with quasicubic {100} faces were obtained, and the composition was determined by inductively coupled plasma analysis. Synchrotron x-ray powder-diffraction measurements performed at BL02B2 beamline in SPring-8 showed the changes in lattice parameters with x that are consistent with the published results,[11] with no sign of impurity phase down to the ~0.1% level. Dielectric and high-T calorimetric measurements confirmed the evolution from relaxor to conventional ferroelectric behavior with increasing x, in agreement with previous studies.[11,12] Also, a single crystal of x =0.32 grown by the Bridgman method was purchased from Sinocera Photonics, Inc. This crystal showed a Schottky anomaly in C_p and Curie contribution in magnetic susceptibility, which corresponded to ~1% of magnetic impurities

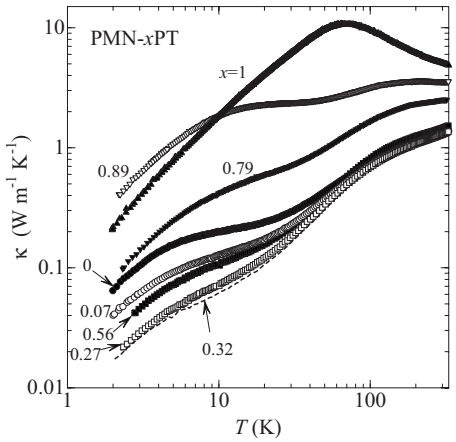

FIG. 1. Thermal conductivity of PMN-PT_x crystals. Typical glasslike and crystalline behaviors are found in $x=0$ and 1, respectively. The data for $x=0.32$ are shown as a dashed line.

(assuming $S=1/2$) in the crystal. However, this kind of impurity is not expected[13,14] to influence the glasslike thermal conductivity,[15] and we present the κ data for this sample. κ measurements were performed in a quantum design PPMS, using the thermal transport option. For the measurement, as-grown crystals were cut into rectangular bars with a typical size of $1.5\times1.5\times3.5$ mm^3, and electrical leads were attached with silver epoxy cured at 200 °C. Several samples were measured for selected compositions, and the reproducibility was checked. C_p measurements down to 0.6 K were performed by the relaxation method using the PPMS. No significant time dependence was observed in the relaxation-time window of ~1 to 100 s at 0.6 K.

In Fig. 1 we show the κ of PMN-PT_x, where the results for PMN ($x=0$) and PT ($x=1$) are reproduced from Ref. 10. The behavior found in PT is typical of crystalline dielectric solids, with a peak at 65 K. On the other hand, the smaller κ found in PMN is both qualitatively and quantitatively identical to the universal behavior[14] found in glasses: at the lowest T below 1 K,[13] which is not covered here, κ varies as T^2 due to the phonon scattering from a distribution of two-level tunneling systems. This is followed by a plateau at ~10 K and another increase at higher T. Figure 1 demonstrates that the evolution from glasslike to crystalline behavior for the solid solution of PMN-PT_x does not occur through a monotonic change in κ. Instead, the smallest κ is found in $x=0.32$ at the MPB, which separates the two composition regions with different systematic behavior. This is our first evidence that thermal properties are intimately coupled to the underlying structures in PMN-PT_x.

Focusing first on $0\leq x\leq0.32$, the systematic behavior in this region is characterized by the suppression of plateau with increasing PT doping (κ at 8 K is shown in Fig. 4), with much smaller variation in κ at higher T. These results immediately recall the almost identical behavior found in partially crystallized glasses[16] and polymers,[17] which have submicrometer-sized crystalline regions dispersed in an amorphous matrix. In these partially crystallized materials, the κ has been explained with the acoustic mismatch model;[18] the mismatch of elastic properties at the interface gives rise to thermal boundary resistance with a T^{-3} dependence, which results in the suppression of plateau. Especially, a systematic study found a clear correlation between the degree of suppression and the concentration of crystalline regions[17] although detailed analysis is made difficult by the complex structure of these systems. Coming back to PMN-PT_x, it is tempting to interpret the results using analogies with the partially crystallized materials. A neutron diffuse scattering study[19] has shown that the average size of PNRs at 10 K increases from 6 nm in $x=0$ to 20 nm in $x=0.1$, and for $x=0.2$ the size of PNRs already reaches the resolution limit of ~35 nm at 300 K. More complicated pictures involving submicrometer-sized ferroelectric domains were observed in scanning force microscopic studies. Shvartsman and Kholkin[6] found PNRs as small as ~5 nm embedded in ferroelectric domains of opposite orientation in $x=0.2$, while Bai *et al.*[7] showed that PNRs gradually transform into ferroelectric domains with increasing x. Because PNRs have an irregular morphology and distribution, it was proposed[7] that their boundaries are not restricted by elastic compatibility, and therefore they are essentially nonstress accommodating. On the other hand, more regular patterns are observed for ferroelectric domains, suggesting the importance of stress accommodation and elastic incompatibility at their boundary.[7] Thus, within the idea of acoustic mismatch model, thermal boundary resistance should be significant at the boundary of ferroelectric domains, while PNRs provide a nanoscale inhomogeneous matrix responsible for the glasslike thermal conduction. Furthermore, the interface between a PNR and the oppositely polarized ferroelectric domain would also contribute to the thermal boundary resistance if their elastic mismatch turns out to be large. In either case, these pictures attribute the suppression of plateau to the rise of ferroelectric domains, which continues up to the MPB. It should be noted that while glasslike κ is found in a number of disordered crystals,[20] PMN-PT_x provides one of the clearest pictures on how κ is affected by the composition and local structures. This feature is potentially useful for the general understanding of glasslike thermal behavior, and more detailed studies on the structural and elastic properties of PNRs and ferroelectric domains are certainly warranted.

For the compositions $0.56\leq x\leq1$, which are in the tetragonal ferroelectric phase, different systematic behavior is observed with PT doping. For these compositions, κ increases gradually with increasing x until it reaches the typical crystalline behavior found in $x=1$. The unusual T dependence of κ, which is especially prominent in $x=0.79$ and 0.89, suggests strong scattering of phonons from structural disorder. It is interesting to note here that a recent neutron-scattering study on $x=0.6$ found damped optic soft phonons near the zone center (the "waterfall" effect) despite the lack of PNRs.[21] These results point to unusually strong impact of chemical disorder on the dynamic properties in tetragonal PMN-PT_x, providing further evidence that this system is far from a simple ferroelectric system.

Heat-capacity measurements provide complementary insights on the evolution from glasslike to crystalline behavior. Figure 2 shows the data below 1.8 K, plotted as C_p/T vs T^2. At the lowest temperatures, C_p obeys the relation $C_p=\gamma T+\beta T^3$, where the intercept γ arises from the two-level systems and the slope β is due to phonons. For PT, the fit

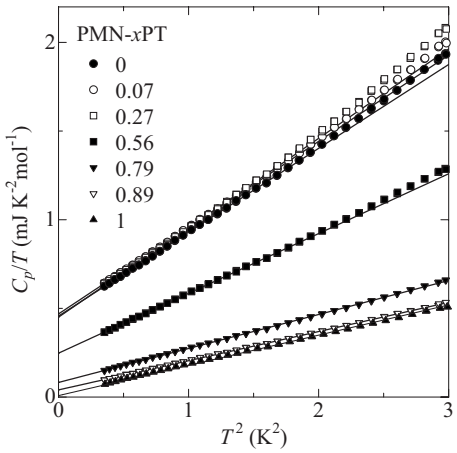

FIG. 2. The low-temperature heat capacity plotted as C_p/T vs T^2. The lines are fits to $C_p=\gamma T+\beta T^3$ as described in the text.

gives γ within experimental error of zero, and the Debye temperature Θ_D obtained from β is in good agreement with the elastic value.[22] For PMN, the fit yields $\gamma=0.46$ mJ K^{-2} mol^{-1} or the two-level density of states $D(\epsilon)=5.9\times10^{21}$ states/eV cm^3, a typical value for amorphous materials.[14] As the elastic Θ_D of PMN is slightly ($\sim$5%) higher than PT,[10,23] the larger β and lower thermal Θ_D in PMN imply the presence of nonacoustic phonon contributions widely found in glasses.[14] Figure 2 shows that these glasslike behaviors of γ and β remain almost constant for x on the left side of the MPB, while these values diminish rapidly for higher x.

In order to examine the lattice dynamics in more detail, we plot C_p/T^3 over a wide T region in Fig. 3. When C_p is plotted this way, the linear term appears as a sharp upturn below 2 K, whereas the T^3 contribution becomes a constant. A broad peak is observed in each x as an additional feature, which is almost identical for $0\leq x\leq0.27$ but becomes lower in height and shifts to higher T for larger x. Interestingly, similar shift in the C_p/T^3 peak is observed between amorphous and crystalline materials.[14] To set energy scales for

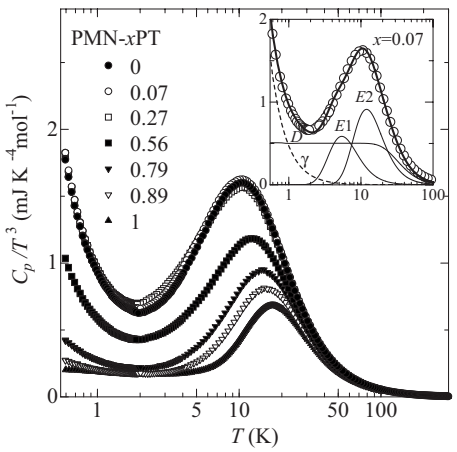

FIG. 3. Heat capacity divided by T^3 for PMN-PT$_x$. The inset shows the contributions from the linear component (γ, dashed line), Debye function D, and two Einstein functions $E1$ and $E2$ for $x=0.07$. Only selected data points are shown in the inset for clarity.

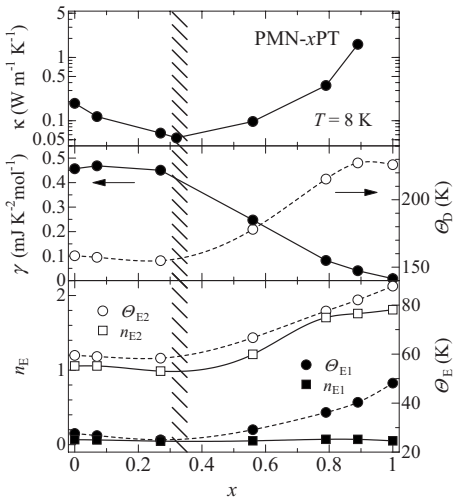

FIG. 4. The x dependence of thermal parameters. (Top) κ at 8 K, (middle) the linear C_p coefficient γ and Debye temperature Θ_D, and (bottom) the temperatures Θ_E and oscillator strengths n_E of two Einstein modes. For Θ_D, the oscillator strength n_D was fixed to 3; Θ_D for $n_D=15$ can be obtained by multiplying the present values by $5^{1/3}$. The hatched region represents the morphotropic phase boundary having a monoclinic symmetry.

these observations, we represent the peak by a combination of two Einstein functions,[24] which are dispersionless modes having characteristic temperatures of Θ_{E1} and Θ_{E2}, and oscillator strengths of n_{E1} and n_{E2} per formula unit, respectively. More specifically, after the γT component is subtracted from the total C_p, the remaining part from 0.6 to 100 K is fitted by a single Debye function and two Einstein functions. To set Θ_D equivalent to the value obtained from β, the oscillator strength of the Debye function is fixed to $n_D=3$.[25] The results for each x are shown in Fig. 4, and individual contributions in the C_p/T^3 plot are shown for $x=0.07$ in the inset of Fig. 3.

For PMN, $\Theta_{E2}=60$ K is consistent with the first peak in the phonon density of states (PDOS) at $\sim$6 meV (1 meV$\approx$11.6 K),[12,26] while the lower Einstein mode with $\Theta_{E1}=28$ K is not apparent in the PDOS due to its much smaller oscillator strength. These parameters remain almost constant for x on the left side of the MPB, indicating that similar PDOS can be expected for these compositions. On the other hand, Θ_D, Θ_{E1}, and Θ_{E2} all increase rapidly with x in the tetragonal phase, leading to the shift of the C_p/T^3 peak as observed in Fig. 3. n_{E2} also increases with x although this effect is not obvious in a C_p/T^3 plot due to the concomitant increase in Θ_{E2}. For PT, $\Theta_{E2}=88$ K agrees well with the peak in PDOS at 8 meV,[27] indicating that the present analysis provides a realistic picture of low-frequency PDOS for the entire series of PMN-PT$_x$.

The above results for PT are fully consistent with the lattice dynamics of crystals: the T^3 term is due to long-wavelength acoustic phonons, and the peak in C_p/T^3 corresponds to the zone-boundary acoustic modes.[27] In contrast, it is not clear how far this picture can be applied to PMN. Although the position of peaks in C_p/T^3 and PDOS is not inconsistent with the zone-boundary acoustic modes,[28] the peak in PDOS becomes higher below room temperature,[26]

possibly being related to PNRs. Moreover, the excess T^3 contribution, as shown by the low thermal Θ_D, implies the presence of additional modes that coexist with acoustic waves[23] down to the lowest frequencies. By analogy with glasses, these additional modes may be found as localized excitations from randomly distributed nanoscale structures, such as PNRs or chemically ordered regions. The weak variation in C_p for $0 \leq x \leq 0.27$ suggests that PNRs are the more likely candidate, as PNRs coexist with ferroelectric domains[6,7] but chemically ordered regions disappear at $x \sim 0.2$.[29] The additional modes are then associated with a broad distribution of soft potentials, whose barriers separate different configurational states of PNRs. In the phenomenological soft potential model of glasses,[30] these potentials also correspond to the two-level tunneling states, and a correlation between γ and the peak in C_p/T^3 is predicted. Interestingly, this is clearly observed in PMN-PT$_x$. It is also interesting to speculate that these low-frequency modes are related to the strong coupling between PNRs and acoustic modes, which was reported in recent neutron-scattering studies.[28,29,31]

While PNRs are apparently needed to saturate the density of low-energy excitations at the level of amorphous solids, the presence of finite γ in the tetragonal phase indicates that quenched chemical disorder can be another source of two-level systems. In many ways, the thermal properties of the tetragonal phase are comparable to a number of disordered crystals where the similarity to glasses is only partial and/or qualitative.[20] The present case of PMN-PT$_x$ provides an example where these properties change smoothly with the composition, which will be valuable for detailed studies on the relationship between disorder and low-energy excitations.

In conclusion, thermal conductivity and heat capacity of PMN-PT$_x$ show remarkable correlation with the phase diagram, demonstrating that thermal properties are intimately coupled to the nanoscale inhomogeneities in relaxor ferroelectric systems.

We acknowledge valuable discussions with S. G. Lushnikov and S. Kojima, and thank S. Takenouchi, T. Yoshida, K. Sasame, H. Kawaji, and T. Atake for assistance in characterizing the crystals. This Rapid Communication was supported by a Grant-in-Aid from JSPS under Grant No. 20740178, and WPI Research Center Initiative on Materials Nanoarchitectonics from MEXT, Japan.

[1] A. A. Bokov and Z.-G. Ye, J. Mater. Sci. **41**, 31 (2006).
[2] E. Dagotto, Science **309**, 257 (2005).
[3] B. Noheda, D. E. Cox, G. Shirane, J. Gao, and Z. G. Ye, Phys. Rev. B **66**, 054104 (2002).
[4] M. Davis, J. Electroceram. **19**, 23 (2007).
[5] I. K. Jeong, T. W. Darling, J. K. Lee, T. Proffen, R. H. Heffner, J. S. Park, K. S. Hong, W. Dmowski, and T. Egami, Phys. Rev. Lett. **94**, 147602 (2005).
[6] V. V. Shvartsman and A. L. Kholkin, Phys. Rev. B **69**, 014102 (2004).
[7] F. Bai, J. Li, and D. Viehland, Appl. Phys. Lett. **85**, 2313 (2004); J. Appl. Phys. **97**, 054103 (2005).
[8] Z. G. Ye, Y. Bing, J. Gao, A. A. Bokov, P. Stephens, B. Noheda, and G. Shirane, Phys. Rev. B **67**, 104104 (2003).
[9] G. Xu, D. Viehland, J. F. Li, P. M. Gehring, and G. Shirane, Phys. Rev. B **68**, 212410 (2003).
[10] M. Tachibana, T. Kolodiazhnyi, and E. Takayama-Muromachi, Appl. Phys. Lett. **93**, 092902 (2008).
[11] A. Kania, A. Slodczyk, and Z. Ujma, J. Cryst. Growth **289**, 134 (2006).
[12] Y. Moriya, H. Kawaji, T. Tojo, and T. Atake, Phys. Rev. Lett. **90**, 205901 (2003).
[13] J. J. De Yoreo, R. O. Pohl, and G. Burns, Phys. Rev. B **32**, 5780 (1985).
[14] *Amorphous Solids: Low Temperature Properties*, edited by W. A. Phillips (Springer, Berlin, 1981).
[15] D.-M. Zhu and P. D. Han, Appl. Phys. Lett. **75**, 3868 (1999).
[16] B. Hanna and R. G. Bohn, J. Am. Ceram. Soc. **74**, 3035 (1991); D. G. Cahill, J. R. Olson, H. E. Fischer, S. K. Watson, R. B. Stephens, R. H. Tait, T. Ashworth, and R. O. Pohl, Phys. Rev. B **44**, 12226 (1991).
[17] C. L. Choy and D. Greig, J. Phys. C **8**, 3121 (1975).
[18] E. T. Swartz and R. O. Pohl, Rev. Mod. Phys. **61**, 605 (1989).
[19] M. Matsuura, K. Hirota, P. M. Gehring, Z. G. Ye, W. Chen, and G. Shirane, Phys. Rev. B **74**, 144107 (2006).
[20] D. G. Cahill, S. K. Watson, and R. O. Pohl, Phys. Rev. B **46**, 6131 (1992).
[21] C. Stock, D. Ellis, I. P. Swainson, G. Xu, H. Hiraka, Z. Zhong, H. Luo, X. Zhao, D. Viehland, R. J. Birgeneau, and G. Shirane, Phys. Rev. B **73**, 064107 (2006).
[22] Thermal and elastic Θ_D of PT are both $\approx$210–225 K or 360–385 K for 3 or 15 oscillator strengths per formula unit, respectively. The latter definition was used in Ref. 10, whereas the former will be used in this Rapid Communication.
[23] A. Y. Wu and R. J. Sladek, Phys. Rev. B **27**, 2089 (1983).
[24] A good fit could not be obtained with a single Einstein mode.
[25] An alternative approach is to use one fixed Debye function with $n_D=3$ for the elastic part and another Debye function for the excess T^3 contribution. However, this approach is not feasible for intermediate x where the elastic value is not known.
[26] S. N. Gvasaliya, S. G. Lushnikov, I. L. Sashin, and T. A. Shaplygina, J. Appl. Phys. **94**, 1130 (2003).
[27] N. Choudhury, E. J. Walter, A. I. Kolesnikov, and C.-K. Loong, Phys. Rev. B **77**, 134111 (2008).
[28] C. Stock *et al.*, J. Phys. Soc. Jpn. **74**, 3002 (2005).
[29] T. Y. Koo, P. M. Gehring, G. Shirane, V. Kiryukhin, S. G. Lee, and S. W. Cheong, Phys. Rev. B **65**, 144113 (2002).
[30] M. A. Ramos and U. Buchenau, in *Tunneling Systems in Amorphous and Crystalline Solids*, edited by P. Esquinazi (Springer, Berlin, 1998); L. Gil, M. A. Ramos, A. Bringer, and U. Buchenau, Phys. Rev. Lett. **70**, 182 (1993).
[31] G. Xu, J. Wen, C. Stock, and P. M. Gehring, Nature Mater. **7**, 562 (2008).